RESEARCH ARTICLE | JUNE 09 2023

Decomposition of the wall-heat flux of compressible boundary layers

Xu Dongdong (徐东东) ✉ 🆔 ; Pierre Ricco 🆔 ; Lian Duan 🆔

Check for updates

CrossMark

View Online

Export Citation

Decomposition of the wall-heat flux of compressible boundary layers

View Online   Export Citation   CrossMark

Dongdong Xu (徐东东),[1,a] (iD) Pierre Ricco,[1] (iD) and Lian Duan[2] (iD)

AFFILIATIONS

[1]Department of Mechanical Engineering, The University of Sheffield, Sheffield S1 3JD, United Kingdom
[2]Department of Mechanical and Aerospace Engineering, The Ohio State University, Columbus, Ohio 43210, USA

[a]Author to whom correspondence should be addressed: dongdong.xu@sheffield.ac.uk

ABSTRACT

We use the method developed by Elnahhas and Johnson ["On the enhancement of boundary layer skin friction by turbulence: An angular momentum approach," J. Fluid Mech. **940**, A36 (2022)] and Xu *et al.* ["Decomposition of the skin-friction coefficient of compressible boundary layers," Phys. Fluids **35**, 035107 (2023)] for the decomposition of the skin-friction coefficient to integrate the mean temperature equation for high-Reynolds-number compressible boundary layers and arrive at an identity for the decomposition of the wall-heat flux. The physical interpretation of the identity and the limitations of this approach are discussed. We perform an integration on the mean temperature equation to obtain an identity that is the heat-transfer analog to the compressible von Kármán momentum integral equation for the skin-friction coefficient. This identity is applied to numerical data for laminar and turbulent compressible boundary layers, revealing that the mean-flow dissipation and production of turbulent kinetic energy given by the Favre–Reynolds stresses dominate the thermal-energy balance. The term related to the growth of the turbulent boundary layer opposes the wall cooling. Other identities for the wall-heat flux, inspired by the method of Fukagata *et al.* ["Contribution of Reynolds stress distribution to the skin friction in wall-bounded flows," Phys. Fluids **14**(11), L73–L76 (2002)], are studied numerically and by asymptotic methods. The terms of these identities depend spuriously on the upper integration bound because this bound is a mathematical quantity used in the derivation. When the bound is asymptotically large, the integral identities simplify to the heat-transfer analog to the von Kármán momentum equation. We also prove that an existing multiple-integration identity reduces to the definition of the wall-heat flux when the number of integrations is asymptotically large. No information about the wall-heat transfer is extracted because the impact of the integration number is nonphysical.

I. INTRODUCTION

The wall-heat transfer of a turbulent boundary layer surpasses that of a laminar boundary layer for the same external flow conditions. In compressible flows, this phenomenon is exacerbated because of the aerothermal heating caused by the viscous effects at very high speeds (Van Driest, 1956; Hopkins and Inouye, 1971). Fundamental and applied research efforts have, therefore, been devoted to the understanding of the heat-transfer mechanism near the wall and to the development of flow control methods, mostly by wall heating and cooling, aimed at protecting the wall from the excessive temperatures (Smits and Dussauge, 2006).

Huang *et al.* (2022) utilized direct numerical simulations to study the severe cooling of hypersonic boundary layers at moderately high Reynolds numbers. The validity of the transformations by Van Driest (1956) and Spalding and Chi (1964), which relate the skin friction of a compressible boundary layer to that of an incompressible boundary layer, was discussed. It was found that the skin-friction values based on those transformations were in good agreement with the correlations at Mach 2.5. However, for hypersonic cases with highly cooled walls, neither of those theories provided a good prediction.

Empirical correlations involving the heat-transfer coefficient and the skin-friction coefficient have also been used. A quantity of interest is the Reynolds analogy factor $R_a = 2S_t/C_f$ (Roy and Blottner, 2006), where S_t is the Stanton number and C_f is the skin-friction coefficient (Hopkins and Inouye, 1971). The experimental measurement of R_a is an immense challenge because of the difficulties related to the high gradients of velocity and temperature at the wall (Goyne *et al.*, 2003).

As alternatives to the direct measurement of wall friction and wall-heat transfer, integral identities obtained from the momentum and energy balances have been developed. The identities for the

incompressible skin-friction coefficient discovered by Fukagata et al. (2002) (FIK) have been widely utilized and extended to evince the impact of the Reynolds stresses on the wall friction. For channel and pipe flows, the wall-shear stress is decomposed in the sum of the laminar wall-shear stress and an integral involving the Reynolds stresses. For free-stream boundary layers, the identity includes an additional term related to the streamwise inhomogeneity of the flow and the components of the decomposition depend on the upper bound of integration (Renard and Deck, 2016; Ricco and Skote, 2022). To deepen the understanding of the skin friction in high-speed flows, the FIK identity was extended to the compressible case by performing a threefold integration (Gomez et al., 2009) and a twofold integration (Wenzel et al., 2022; Xu et al., 2022). The wall-heat transfer was also investigated by using the FIK decomposition method. Zhang and Xia (2020) utilized the twofold integration method to study the heat-transfer integral equation for turbulent channel flows. For free-stream boundary layers, Wenzel et al. (2022) (WGK) and Xu et al. (2022) also used twofold integration identities to investigate the decomposition of the wall-heat transfer of compressible flows. The impact of the integration upper bound in the heat-transfer integral formula was discussed by WGK. Barone et al. (2022) studied the decomposition of the internal energy by using the method of WGK to study hypersonic turbulent boundary layers.

Renard and Deck (2016) (RD) proposed an alternative identity based on the mean kinetic-energy equation to give a quantitative physical explanation to the impact of the energy budget on the skin-friction coefficient of boundary-layer flows. The RD method was extended by Sun et al. (2021) to study the heat-transfer coefficient of compressible boundary layers. This approach was also utilized by Tong et al. (2022a; 2022b). The RD method, in the wall-friction case, offers a clear physical interpretation for each term in the identity and bears no issues related to the upper bound because the wall-normal integration is unbounded. However, as discussed in the studies of Zhang et al. (2022) and Xu et al. (2022), unlike the RD decomposition for the skin-friction coefficient, the physical interpretation of the terms in the RD identity for the wall-heat flux is not clear. The RD and FIK-like identities for the skin-friction and wall-heat transfer coefficients in the case of free-stream boundary layers do not isolate the laminar coefficients, as, instead, successfully done in the original FIK identity for channel and pipe flows.

Elnahhas and Johnson (2022) (EJ) derived an identity for the decomposition of the skin-friction coefficient of incompressible boundary layers. They identified a quantity, function of the streamwise direction, as a preferred wall-normal position inside the boundary layer around which the angular momentum exerted by the flow is computed. The wall-normal integration is unbounded and the identity isolates the skin friction of the laminar Blasius boundary layer. Following the same theoretical method of EJ, Kianfar et al. (2022b) investigated the decomposition of the Stanton number in incompressible turbulent boundary layers. Their integral equation for the heat-transfer coefficient bears full analogy with the integral equation for the skin-friction coefficient when the Prandtl number is unity. Xu et al. (2023) used EJ's method to study the wall friction of compressible boundary layers and also investigated the impact of the wall-normal integration bound in the existing compressible FIK-like identities. Kianfar et al. (2022a) obtained an identity similar to that of Xu et al. (2023), although the impact of the change of viscosity due to the temperature gradient on the skin friction was treated differently in the two formulations. The wall-normal gradient of the mean viscosity was

isolated in an integral term by Xu et al. (2023), while a reference mean viscosity was used by Kianfar et al. (2022a).

In this paper, we study the impact of the energy-budget terms on the wall-heat flux of compressible laminar and turbulent boundary layers. In Sec. II, the Favre-averaged temperature equation is discussed. In Sec. III, we integrate the Favre-averaged temperature equation, following the method of EJ and Xu et al. (2023) for the decomposition of the wall friction. The physical interpretation and limitations of the resulting identity are discussed. In Sec. IV, we integrate the temperature equation to obtain the heat-transfer analog to the von Kármán momentum integral equation. Numerical results based on the latter integral identity are presented for compressible laminar and turbulent boundary layers. An evaluation of the existing FIK-like identities for the wall-heat flux is found in Sec. V, where the focus is on the dependence of those relations on the upper integration bound and the number of successive integrations. Conclusions are presented in Sec. VI.

II. THE TEMPERATURE BALANCE EQUATION

We consider a two-dimensional compressible boundary layer over a flat plate, where x^*, y^*, and z^* are the streamwise, the wall-normal, and the spanwise directions, respectively. The flat plate is at $y^* = 0$, and the leading edge of the plate is at $x^* = 0$. The wall temperature T_w^* is constant (the subscript w denotes quantities at the wall). The Navier–Stokes equations and the energy equation are scaled by the uniform free-stream velocity $\mathcal{U}_\infty^*$ as the reference velocity and a length $\mathcal{L}^*$ as the reference length scale. The temperature T^*, the density ρ^*, the dynamic viscosity μ^*, and the thermal conductivity κ^* are scaled by their respective constant free-stream values, T_∞^*, ρ_∞^*, μ_∞^*, and κ_∞^*. The time t^* and the pressure p^* are scaled by $\mathcal{L}^*/\mathcal{U}_\infty^*$ and $\rho_\infty^* \mathcal{U}_\infty^{*2}$, respectively. The specific heat capacity c_p^* is scaled by U_∞^{*2}/T_∞^*. The asterisk $*$ indicates dimensional quantities, while quantities without any symbol are nondimensional.

Reynolds averaging a quantity q over z along a distance $\mathcal{L}_z$ and over t for a time interval $\mathcal{T}$ is defined as

$$\bar{q}(x,y) = \frac{1}{\mathcal{L}_z \mathcal{T}} \int_0^{\mathcal{T}} \int_0^{\mathcal{L}_z} q(x,y,z,t) \mathrm{d}z \mathrm{d}t. \quad (2.1)$$

A Favre-averaged quantity is defined as $\langle q \rangle = \overline{\rho q}/\bar{\rho}$ (Favre, 1965; 1992). The flow is decomposed as follows:

$$q(x,y,z,t) = \bar{q}(x,y) + q'(x,y,z,t) = \langle q \rangle(x,y) + q''(x,y,z,t). \quad (2.2)$$

The Favre-averaged continuity, momentum and energy equations for compressible, statistical two-dimensional flows are (Adumitroaie et al., 1999)

$$\frac{\partial \bar{\rho} \langle u_j \rangle}{\partial x_j} = 0,$$

$$\frac{\partial \bar{\rho} \langle u_i \rangle \langle u_j \rangle}{\partial x_j} + \frac{\partial \bar{\rho} \langle u_i'' u_j'' \rangle}{\partial x_j} = -\frac{\partial \bar{p}}{\partial x_i} + \frac{\partial \bar{\sigma}_{ji}}{\partial x_j},$$

$$\frac{\partial \bar{\rho} \langle e \rangle \langle u_j \rangle}{\partial x_j} + \frac{\partial \bar{\rho} \langle e'' u_j'' \rangle}{\partial x_j} = -\frac{1}{(\gamma-1)RePr\mathcal{M}_\infty^2} \frac{\partial \bar{q}_j(T)}{\partial x_j} \quad (2.3)$$

$$+ \frac{\partial}{\partial x_j}(\overline{u_i \sigma_{ji}} - \overline{pu_j}),$$

where e is the total energy,

$$e = \frac{T}{\gamma(\gamma-1)\mathcal{M}_\infty^2} + \frac{u_j u_j}{2} = \frac{c_p T}{\gamma} + \frac{u_j u_j}{2}, \qquad (2.4)$$

$\mathscr{q}_j(T) = -\kappa\partial T/\partial x_j$ is the heat flux, and the Mach number, the Reynolds number, and the Prandtl number are defined as follows:

$$\mathcal{M}_\infty = \frac{\mathcal{U}_\infty^*}{\sqrt{\gamma\mathcal{R}^* T_\infty^*}}, \quad Re = \frac{\rho_\infty^* \mathcal{U}_\infty^* \mathcal{L}^*}{\mu_\infty^*}, \quad \text{and} \quad Pr = \frac{c_{p\infty}^* \mu_\infty^*}{\kappa_\infty^*}, \qquad (2.5)$$

where the ratio of specific heats is $\gamma = c_p^*/c_v^* = 1.4$, c_v^* denotes the specific heat capacity at constant volume and the ideal gas constant is $\mathcal{R}^* = 287.05\,\mathrm{Jkg^{-1}K^{-1}}$. The stress tensor is $\sigma_{ij} = (2\mu/Re)[S_{ij} - (S_{kk}/3)\delta_{ij}]$, where the stress rate is $S_{ij} = (\partial u_i/\partial x_j + \partial u_j/\partial x_i)/2$, and δ_{ij} is the Kronecker delta. The Einstein summation convention is adopted to any Latin suffix occurring twice in an expression. The Prandtl number and the specific heat capacities are constant and, therefore, the scaled thermal conductivity κ is equal to the scaled dynamic viscosity μ.

From the total energy balance, expressed by the total energy equation in Eq. (2.3) and utilized in detail by Van Driest (1951), various forms of the energy equation can be derived, such as the total enthalpy/energy equation (WGK, Sun *et al.*, 2021), the kinetic equation (Fan *et al.*, 2022), the enthalpy equation, the internal equation (Barone *et al.*, 2022; Xu *et al.*, 2022), and the temperature equation. It is instructive to discuss which of those forms of the energy balance is the most appropriate one for our analysis. As the total enthalpy/energy balance does not separate the internal energy and the kinetic energy, the total enthalpy/energy equation does not uncover the energy exchanges among the components of the total energy, such as the heat generation by the mean and turbulent viscous dissipations (Barone *et al.*, 2022). The internal energy equation or the temperature equation is instead more suited to study the heat transfer within the flow, as they contain terms related to the generation and transfer of internal energy. We choose to utilize the mean temperature equation in our heat-transfer study for three main reasons. First, the temperature, which appears explicitly in the equation as the main unknown, can be measured directly in an experiment. Second, the absence of the turbulent dissipation term is an advantage because this quantity is very complicated to measure experimentally as it involves correlations of the instantaneous spatial gradients of the velocity fluctuations [refer to Andreopoulos and Honkan (2001) for incompressible boundary layers and Lapsa and Dahm (2011) for compressible boundary layers]. Third, the turbulent production term appears in the equation in lieu of the turbulent dissipation term, as shown in Eq. (14) of Barone *et al.* (2022) and Eq. (7–95d) in White (2006). This occurrence is convenient because the turbulent production involves the Favre–Reynolds stresses and the mean-velocity gradient, which are quantities that are more readily obtainable experimentally than the turbulent dissipation. Furthermore, the direct role of the Favre–Reynolds stresses on the heat balance is revealed when the production of turbulent kinetic energy is retained, while it would not be available if the total energy equation were utilized.

In our integral analysis, we express the mean wall-heat flux as $\bar{\mathscr{q}}_w = -\mu_w\partial\bar{T}/\partial y|_{y=0}$. It is useful to discuss why we choose not to scale the wall-heat flux by using the Stanton number or the Nusselt number. The Stanton number was used by Kianfar *et al.* (2022b) in their identity involving the wall-heat transfer in incompressible turbulent boundary layers. The Stanton number for compressible boundary layers, given in Eq. (6.63) in Anderson (2000), is defined as follows:

$$\begin{aligned}\mathcal{S}_t &= \frac{\kappa_w^*}{\rho_\infty^* \mathcal{U}_\infty^* c_{p\infty}^* (T_{ad}^* - T_w^*)}\frac{\partial\bar{T}^*}{\partial y^*}\bigg|_{y^*=0}\\ &= \frac{\kappa_w}{(T_{ad}-T_w)Re\,Pr}\frac{\partial\bar{T}}{\partial y}\bigg|_{y=0}\\ &= \frac{-\bar{\mathscr{q}}_w}{(T_{ad}-T_w)Re\,Pr},\end{aligned} \qquad (2.6)$$

where T_{ad} denotes the adiabatic wall temperature, $\bar{\kappa} = \kappa_w$ at $y=0$ since the wall is isothermal ($\partial\bar{T}^*/\partial y^*$ is instead different from $\partial T^*/\partial y^*$ as the temperature-gradient disturbances are not null at the wall). The Nusselt number is defined as follows:

$$\mathcal{N}_u = \frac{x^*\kappa_w^*}{\kappa_\infty^*(T_{ad}^* - T_w^*)}\frac{\partial\bar{T}^*}{\partial y^*}\bigg|_{y^*=0} = \mathcal{S}_t Re_x Pr, \qquad (2.7)$$

where $Re_x = \rho_\infty^* U_\infty^* x^*/\mu_\infty^*$. It is noted that, as discussed in Anderson (2000) on p. 298, the Stanton and Nusselt numbers have finite values at any Mach number in the adiabatic wall case despite their indefinite forms, given by $\partial\bar{T}^*/\partial y^*|_{y^*=0} = 0$ at the numerator and $T_{ad}^* - T_w^* = 0$ at the denominator. As we are interested in the physics of heat transfer in boundary layers, it is important in our study to obtain an integral relation where the constituent terms balance out to produce a null wall-heat flux in the adiabatic wall case and not a finite value as in the case of the Stanton and Nusselt numbers. The Stanton and Nusselt numbers are more useful in empirical correlations as the wall-heat convection coefficient can be readily computed as a function of Re_x, Pr, and $\mathcal{M}_\infty$.

In deriving the mean temperature equation used in our analysis, we follow Van Driest (1951), who simplified the total energy equation (2.3). The disturbance terms $\overline{u'^2}$ and $\overline{v'^2}$ are assumed to be negligibly small compared to $\bar{u}^2$ and all the triple correlations are also neglected. In the limit of large Reynolds number, the boundary layer is assumed to be thin and, therefore, $\partial\overline{(\rho u)'T'}/\partial x \ll \partial\overline{(\rho u)'T'}/\partial y$ and $\partial\bar{u}/\partial x$, $\partial\bar{v}/\partial y$, $\partial\bar{v}/\partial x$ are all negligible with respect to $\partial\bar{u}/\partial y$. Van Driest (1951) neglected the mean heat conduction and the viscous heat generation, but we retain these effects because our focus is on the large heat flux at the wall and on the heat generation, which is significant at high Mach numbers. We have also verified numerically that term $\partial(\overline{\mu'\partial T'/\partial y})/\partial y$ is very small in the boundary layer (it is zero at the isothermal wall because $\mu' = 0$). The flow is free from pressure-gradient effects, which could be studied by retaining the term $\bar{u}\,d\bar{p}/dx$. The resulting equation, also given as (7–95d) in White (2006), rewritten in Favre-averaged form, reads

$$\begin{aligned}&\frac{\partial\bar{\rho}\langle T\rangle\langle u\rangle}{\partial x} + \frac{\partial\bar{\rho}\langle T\rangle\langle v\rangle}{\partial y} + \frac{\partial\bar{\rho}\langle v''T''\rangle}{\partial y} - \frac{1}{RePr}\frac{\partial}{\partial y}\left(\bar{\mu}\frac{\partial\bar{T}}{\partial y}\right)\\ &- \frac{\mathcal{M}_\infty^2(\gamma-1)}{Re}\bar{\mu}\left(\frac{\partial\bar{u}}{\partial y}\right)^2 + \mathcal{M}_\infty^2(\gamma-1)\bar{\rho}\langle u''v''\rangle\frac{\partial\bar{u}}{\partial y} = 0. \quad (2.8)\end{aligned}$$

The first two terms represent the convective transport by the mean flow, the third term denotes the turbulent heat transport, the fourth term is the mean heat conduction, the fifth term is the heat

generation caused by the mean velocity gradient, and the last term is the production of turbulent kinetic energy. The turbulent kinetic energy budget for a hypersonic boundary layer [Fig. 14 in Zhang *et al.* (2018)] shows that the production of turbulent kinetic energy balances the viscous dissipation of turbulent kinetic energy into heat.

III. EXTENSION OF ELNAHHAS–JOHNSON METHOD TO THE WALL-HEAT FLUX BALANCE

By using the temperature equation (2.8), we extend the method of EJ and Xu *et al.* (2023) for the decomposition of the wall-friction coefficient to derive an identity for the decomposition of the wall-heat flux. Subtracting the continuity equation, given by the first Eq. (2.3), from Eq. (2.8) leads to the temperature deficit equation,

$$\frac{\partial(\langle T\rangle - 1)\bar{\rho}\langle u\rangle}{\partial x} + \frac{\partial(\langle T\rangle - 1)\bar{\rho}\langle v\rangle}{\partial y} + \frac{\partial\bar{\rho}\langle v''T''\rangle}{\partial y} - \frac{1}{RePr}\frac{\partial}{\partial y}\left(\bar{\mu}\frac{\partial\bar{T}}{\partial y}\right)$$
$$- \frac{\mathcal{M}_\infty^2(\gamma-1)}{Re}\bar{\mu}\left(\frac{\partial\bar{u}}{\partial y}\right)^2 + \mathcal{M}_\infty^2(\gamma-1)\bar{\rho}\langle u''v''\rangle\frac{\partial\bar{u}}{\partial y} = 0. \quad (3.1)$$

The energy integral equation is obtained by multiplying (3.1) by $y - \mathcal{L}$ and integrating from 0 to ∞, where $\mathcal{L}$ is a length to be determined. Dividing the resulting expression by $\mathcal{L}/(Re\,Pr)$ leads to

$$\bar{\mathcal{q}}_w = -\mu_w\frac{\partial\bar{T}}{\partial y}\Bigg|_{y=0}$$
$$= \underbrace{-\frac{1}{\mathcal{L}}}_{\bar{\mathcal{q}}_l} + \underbrace{\frac{\mu_w T_w}{\mathcal{L}} + \frac{1}{\mathcal{L}}\int_0^\infty\frac{\partial\bar{\mu}}{\partial y}\bar{T}\,\mathrm{d}y}_{\bar{\mathcal{q}}_{\bar{\mu}}}$$
$$\underbrace{- Pr\mathcal{M}_\infty^2(\gamma-1)\int_0^\infty\left(1-\frac{y}{\mathcal{L}}\right)\bar{\mu}\left(\frac{\partial\bar{u}}{\partial y}\right)^2\mathrm{d}y}_{\bar{\mathcal{q}}_u}$$
$$\underbrace{+ RePr\mathcal{M}_\infty^2(\gamma-1)\int_0^\infty\left(1-\frac{y}{\mathcal{L}}\right)\bar{\rho}\langle u''v''\rangle\frac{\partial\bar{u}}{\partial y}\,\mathrm{d}y}_{\bar{\mathcal{q}}_{tur}}$$
$$\underbrace{+ \frac{RePr}{\mathcal{L}}\int_0^\infty\bar{\rho}\langle v''T''\rangle\,\mathrm{d}y}_{\bar{\mathcal{q}}_h}$$
$$\underbrace{+ RePr(T_w-1)\frac{\mathrm{d}\theta_{\mathcal{L}}^T}{\mathrm{d}x} - \frac{RePr(T_w-1)}{\mathcal{L}}\left(\theta^T - \theta_{\mathcal{L}}^T\right)\frac{\mathrm{d}\mathcal{L}}{\mathrm{d}x}}_{\bar{\mathcal{q}}_{\theta^T}}$$
$$\underbrace{+ \frac{RePr(T_w-1)}{\mathcal{L}}\theta_v^T}_{\bar{\mathcal{q}}_{\theta_v^T}}, \quad (3.2)$$

where

$$\theta^T(x) \equiv \int_0^\infty\frac{\langle T\rangle - 1}{T_w - 1}\bar{\rho}\langle u\rangle\,\mathrm{d}y, \quad (3.3)$$

is the enthalpy thickness,

$$\theta_{\mathcal{L}}^T(x) \equiv \int_0^\infty\left(1-\frac{y}{\mathcal{L}}\right)\frac{\langle T\rangle - 1}{T_w - 1}\bar{\rho}\langle u\rangle\,\mathrm{d}y, \quad (3.4)$$

is the thermal boundary-layer thickness defined by $\mathcal{L}$, and

$$\theta_v^T \equiv \int_0^\infty\frac{\langle T\rangle - 1}{T_w - 1}\bar{\rho}\langle v\rangle\,\mathrm{d}y, \quad (3.5)$$

is the thermal thickness related to the mean wall-normal velocity. Note that, as in the identity (14) derived by Kianfar *et al.* (2022b) for the incompressible heat-transfer case, $T_w - 1$ appears as a multiplicative factor in the terms $\bar{\mathcal{q}}_{\theta^T}$ and $\bar{\mathcal{q}}_{\theta_v^T}$ in order to define the thicknesses θ^T, $\theta_{\mathcal{L}}^T$, and θ_v^T.

In Eq. (3.2), term $\bar{\mathcal{q}}_l$ is the laminar wall-heat flux, term $\bar{\mathcal{q}}_{\bar{\mu}}$ indicates the contribution of the mean flow due to the variation of viscosity, term $\bar{\mathcal{q}}_u$ represents the mean-flow dissipation, and term $\bar{\mathcal{q}}_{tur}$ quantifies the production of turbulent kinetic energy by the Favre–Reynolds stresses. Term $\bar{\mathcal{q}}_h$ is due to the turbulent heat flux, while the remaining terms are related to the nonparallel mean convective transport, i.e., $\bar{\mathcal{q}}_{\theta_v^T}$ is due to the wall-normal velocity, and $\bar{\mathcal{q}}_{\theta^T}$ is due to the spatial evolution of the momentum thickness and the length $\mathcal{L}$. When the heat-transfer identity (3.2) is compared to the compressible skin-friction identity, given by Eq. (2.15) in Xu *et al.* (2023), we note that the first term of $\bar{\mathcal{q}}_{\bar{\mu}}$ in Eq. (3.2) bears no analog in the skin-friction identity because the no-slip condition renders that term null in the momentum case, while T_w is always a finite quantity. Analogs to the terms proportional to the Mach number in Eq. (3.2), i.e., $\bar{\mathcal{q}}_u$ and $\bar{\mathcal{q}}_{tur}$, are absent in the skin-friction identity because no generation of momentum occurs in that case.

Similar to the derivation of the skin-friction identities [EJ, Xu *et al.* (2023)], the key step is to choose the length scale $\mathcal{L}(x)$ in such a way to render $\bar{\mathcal{q}}_l$, the first term on the right-hand side of Eq. (3.2), equal to the wall-heat flux of the laminar boundary layer. This procedure is discussed in the Appendix. The length scale is found to be

$$\mathcal{L}(x) = \frac{\sqrt{2x/Re}\,T_w}{\mu_w\mathrm{d}T/\mathrm{d}\eta|_{\eta=0}}, \quad (3.6)$$

where η is the similarity co-ordinate for the laminar Blasius flow defined in Eq. (A2).

We now discuss a number of issues that arise when identity (3.2) is used for compressible boundary layers. We first note that, in the adiabatic wall case, even though the wall-heat flux is null, the exchanges of thermal energy within the boundary layer are nevertheless significant, especially in the hypersonic regime. However, in the adiabatic wall case, the length (3.6) is infinite because $\mathrm{d}T/\mathrm{d}\eta|_{\eta=0}$ is zero and, therefore, terms $\bar{\mathcal{q}}_l$, $\bar{\mathcal{q}}_{\bar{\mu}}$, $\bar{\mathcal{q}}_h$, and $\bar{\mathcal{q}}_{\theta^T}$ in Eq. (3.2) vanish because $\mathcal{L}$ appears at the denominators in those terms. The most relevant loss of information is certainly given by the absence of $\bar{\mathcal{q}}_h$, i.e., it is not possible to quantify the role of the turbulent transport term $\langle v''T''\rangle$ in the heat-transfer balance.

We pointed out in Sec. II that scaling the wall-heat flux by the Stanton number or the Nusselt number is not suitable because, in the adiabatic wall case, these numbers are finite, while $\bar{\mathcal{q}}_w = 0$ and, therefore, the physics of wall-heat transfer is not represented properly. If these nondimensional numbers were nevertheless used to express the wall-heat flux in identity (3.2), the adiabatic wall case could only be treated mathematically in the limit of vanishingly small wall-heat flux because $\mathcal{S}_t$ would be proportional to the ratio of $\mathrm{d}T/\mathrm{d}\eta|_{\eta=0}$ and $T_{ad} - T_w$, which are both null.

Further problems arise for a hypersonic boundary layer subjected to intense wall cooling. In this case, $\mathscr{L}$ becomes very small because, in Eq. (3.6), T_w is small at the numerator and $dT/d\eta|_{\eta=0}$ is large at the denominator. In the limit of asymptotically small $\mathscr{L}$, all the terms in Eq. (3.2) become asymptotically large, and it is thus not clear whether the balance expressed in the identity is representative of the heat-transfer physics.

Thoughts are also due about the interpretation of term $\bar{q}_h$ in Eq. (3.2), involving the turbulent transport term $\langle v''T''\rangle$. As amply verified over a large range of Mach numbers and wall-heat-transfer conditions, the turbulent Prandtl number is between 0.8 and 1 across the boundary layer (Huang *et al.*, 2022), which means that $-\langle v''T''\rangle$ and $\partial\langle T\rangle/\partial y$ have the same sign at any wall-normal location because $-\langle u''v''\rangle$ and $\partial\langle u\rangle/\partial y$ are always positive. In hypersonic wall-cooling conditions, $-\langle v''T''\rangle$ is positive near the wall and, thus, gives a direct contribution to the positive wall-temperature gradient there, analogous to the role played by the Favre–Reynolds stresses $-\langle u''v''\rangle$ on the wall friction. However, beyond this thin heat-conduction thickness, $\partial\langle T\rangle/\partial y$ changes sign because of the viscous heat-generation effect, and so does $-\langle v''T''\rangle$. As the Mach number grows, the near-wall heat-conduction region becomes progressively thinner than the core of the thermal boundary layer where the heat generation dominates the energy balance. It follows that the integral contribution of $\bar{\rho}\langle v''T''\rangle$ near the wall may be less significant than that in the boundary-layer core. The sign of $\bar{q}_h$, i.e., the wall-normal integrated effect of $\bar{\rho}\langle v''T''\rangle$, may thus be positive, i.e., opposite to that of the cooling heat transfer at the wall. The integration may obscure the impact of $\langle v''T''\rangle$ near the wall and lead to the conclusion that $\langle v''T''\rangle$ is not relevant for the wall-heat transfer mechanism. Further research on the integrated effect of $\langle v''T''\rangle$ is certainly needed.

Another issue concerns the enthalpy thickness θ^T, defined in Eq. (3.3), and appearing in term $\bar{q}_{\theta^T}$ of the identity (3.2). Kays and Crawford (1993) and Schlichting and Gersten (2016) suggest the use of the enthalpy thickness as a measure of the wall-normal extent of the thermal boundary layer for low-speed flows, i.e., for flows where the exchange of thermal energy is only produced by the wall-heat flux and the viscous heat-generation is negligible. As shown in Fig. 1, in wall-cooling cases at $\mathcal{M}_\infty = 0$ and 2.5, the ratio $(\langle T\rangle - 1)/(T_w - 1)$ is always positive and, thus, the integral defining θ^T is representative of the thermal-layer thickness. However, in the case of a hypersonic boundary layer, where heat generation by viscous dissipation plays a leading role in the energy balance, the enthalpy thickness can fail to represent the thermal-layer thickness. We note that, at high Mach

numbers with $T_w = 1$, the thermal boundary layer does exist, but the enthalpy thickness is not defined because of the singular denominator $T_w - 1$. Furthermore, Fig. 1 shows that, in a laminar case with $\mathcal{M}_\infty = 10.9$ and intense wall cooling ($T_w < 1$), the ratio $(\langle T\rangle - 1)/(T_w - 1)$ is negative except very near the wall. Since $\bar{\rho}$ and $\langle u\rangle$ are always positive, it follows that θ^T, the integrated product of these three quantities, is negative and, thus, it does not represent the wall-normal region where temperature gradients are finite. We have indeed not been able to find in the literature any study where the enthalpy thickness has been employed to investigate hypersonic wall-bounded flows in cooling conditions. We conclude that the use of the enthalpy thickness in the identity (3.2) is questionable in these extreme cases. Similar reasoning pertains to the other two thermal thicknesses involved in the integral balance (3.2), i.e., $\theta^T_{\mathscr{L}}$ and θ^T_v.

In the case of wall heating, the wall-heat flux $\bar{q}_w$ is positive and, thus, the length $\mathscr{L}$ is negative as it has the same sign of $dT/d\eta|_{\eta=0}$. The Reynolds number based on $\mathscr{L}$, as defined in EJ, Kianfar *et al.* (2022b) and Xu *et al.* (2023), would be negative and, therefore, meaningless. Furthermore, a negative $\mathscr{L}$ refers to a wall-normal location under the wall surface and, therefore, it is questionable how the physical interpretation of the wall-friction identity based on the angular momentum, put forward by EJ, could be reinterpreted in this case. At this point, it is not clear how the angular-momentum interpretation, used by EJ to explain the momentum balance, could be extended in the wall-heat flux case for any wall boundary conditions and Mach numbers.

One idea to avoid the negative $\mathscr{L}$ would be to use the same $\mathscr{L}$ adopted in the derivation of the identity for the skin-friction coefficient. At first, this choice appears to be physically reasonable because the transfers of momentum and thermal energy are fully coupled in the compressible regime. However, the first term on the right-hand side of identity (3.2) would not represent the contribution of the laminar wall-heat flux. This result is a major shortcoming because the isolation of the laminar contribution is a unique feature of EJ's method.

Most of the issues just discussed do not, however, pertain to the identity (14) derived by Kianfar *et al.* (2022b), who investigated the heat transfer in an incompressible boundary layer. In that case, the energy equation in the incompressible regime is an independent transport equation, decoupled from the continuity and momentum equations, as the temperature behaves as a passive scalar. We note, for example, that the identity equation (14) in Kianfar *et al.* (2022b) does not involve the mean-flow viscosity term $-Re^{-1}\bar{\mu}(\partial\bar{u}/\partial y)^2$ and the Favre–Reynolds stress term $\bar{\rho}\langle u''v''\rangle\partial\bar{u}/\partial y$ because those terms are
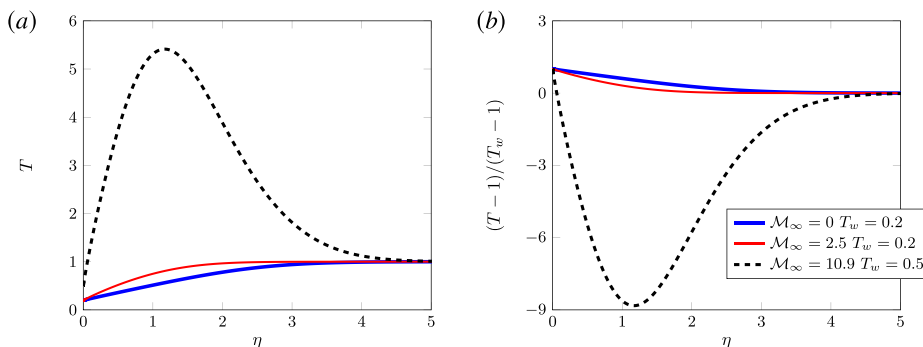

FIG. 1. (a) Temperature distributions of laminar boundary layers at different Mach numbers and wall-cooling conditions. (b) Ratio $(T - 1)/(T_w - 1)$ for the same flow conditions.

Legend:
$\mathcal{M}_\infty = 0 \; T_w = 0.2$
$\mathcal{M}_\infty = 2.5 \; T_w = 0.2$
$\mathcal{M}_\infty = 10.9 \; T_w = 0.5$

proportional to the Mach number, which is null for the flow conditions studied by Kianfar et al. (2022b).

IV. THE DIRECT INTEGRATION METHOD

A compressible temperature integral equation is obtained by integrating (3.1) from 0 to ∞ and multiplying both sides by $RePr$. The wall-heat flux becomes

$$
\begin{aligned}
\bar{\mathscr{q}}_w &= -\mu_w \frac{\partial \bar{T}}{\partial y}\bigg|_{y=0} \\
&= \underbrace{RePr \frac{\mathrm{d}}{\mathrm{d}x} \int_0^\infty (\langle T \rangle - 1)\bar{\rho}\langle u \rangle \mathrm{d}y}_{\bar{\mathscr{q}}_\theta^T} \\
&\quad \underbrace{- Pr\mathcal{M}_\infty^2(\gamma - 1) \int_0^\infty \bar{\mu}\left(\frac{\partial \bar{u}}{\partial y}\right)^2 \mathrm{d}y}_{\bar{\mathscr{q}}_u} \\
&\quad + \underbrace{RePr\mathcal{M}_\infty^2(\gamma - 1) \int_0^\infty \bar{\rho}\langle u''v'' \rangle \frac{\partial \bar{u}}{\partial y} \mathrm{d}y}_{\bar{\mathscr{q}}_{tur}}.
\end{aligned} \tag{4.1}
$$

To the best of our knowledge, identity (4.1) has never been used to study the wall-heat flux. We note that term $\bar{\mathscr{q}}_\theta^T$ is written without using the enthalpy thickness because this quantity may not represent the thickness of the thermal boundary layer in some hypersonic cases, as discussed in Sec. III. Equation (4.1) for the wall-heat transfer is analogous to the von Kármán momentum integral equation for the skin friction,

$$
C_f = 2\frac{\mathrm{d}\theta}{\mathrm{d}x}, \tag{4.2}
$$

where $C_f = 2\tau_w^*/(\rho_\infty^* \mathcal{U}_\infty^{*2})$ is the skin-friction coefficient, τ_w^* is the time and spanwise-averaged wall-shear stress, and $\theta = \int_0^\infty \bar{\rho}\langle u \rangle (1 - \langle u \rangle)\mathrm{d}y$ is the momentum thickness. Identity (4.2) is valid for compressible boundary layers with a uniform free-stream flow and in the high-Reynolds-number limit [refer to Eqs. (7)–(60) in White (2006) for the generalized case with pressure variations and nonuniform free stream]. Identity (4.1) is also obtained by taking the limit $\mathscr{L} \to \infty$ in Eq. (3.2), as discussed in the Appendix. The Favre–Reynolds stresses appear in Eq. (4.1), while they are absent in the von Kármán momentum equation (4.2). Their role is, however, different in the two cases, i.e., production of kinetic energy (balanced by the heat generation via viscous turbulent dissipation) in Eq. (4.1) and direct contribution to the skin friction in the momentum equation, from which Eq. (4.2) is derived. Analogous to the von Kármán momentum equation, the turbulent transport correlation $\langle v''T'' \rangle$ is absent from the balance (4.1) and the laminar contribution to the wall-heat transfer is not isolated. The domain of integration in Eq. (4.1) is unbounded, while the upper bound instead plays a role in the FIK-like identities discussed in Sec. V.

For incompressible boundary layers, i.e., $\mathcal{M}_\infty \to 0$, the wall-heat flux becomes

$$
\bar{\mathscr{q}}_w = RePr(T_w - 1)\frac{\mathrm{d}\theta^T}{\mathrm{d}x}, \tag{4.3}
$$

usually written in the literature as $\mathcal{S}_t = \mathrm{d}\theta^T/\mathrm{d}x$ (Kays and Crawford, 1993) [note that T_{ad} in Eq. (2.6) simplifies to unity when $\mathcal{M}_\infty \to 0$]. The enthalpy thickness θ^T may be used in Eq. (4.3) because it

represents the thickness of the thermal boundary layer in the incompressible case (Kays and Crawford, 1993). The mean-flow dissipation and the Favre–Reynolds stresses give no contribution to the wall-heat flux in the incompressible case. For hypersonic boundary layers at very large Mach number $\mathcal{M}_\infty \gg 1$, the first and second terms on the right-hand side of Eq. (4.1) are of order $O(\mathcal{M}_\infty^2)$. However, the first term on the right-hand side of Eq. (4.1) cannot be neglected because it involves the mean temperature, which also grows with $\mathcal{M}_\infty^2$. In the hypersonic limit $\mathcal{M}_\infty \gg 1$, the boundary-layer assumption may not be valid because of the thickening of the boundary layer (Anderson, 2000) and, therefore, the terms neglected in the derivation of identity (4.1) may have to be reinstated.

An alternative von Kármán-type integral equation for the wall-heat transfer can be derived by using the total energy equation, i.e., (7–103) in White (2006), showing that the wall-heat transfer is induced by the loss or gain of total energy. The main difference between (7–103) in White (2006) and our (4.1) is the neglect of our mean-flow dissipation term $\bar{\mathscr{q}}_u$ and the Favre–Reynolds-stress production term $\bar{\mathscr{q}}_{tur}$, which cannot be disregarded when $\mathcal{M}_\infty = O(1)$. The thermal-energy-integral equation (10.94) in Schlichting and Gersten (2016) is only valid for laminar boundary layers, whereas our identity (4.1) can be utilized for high-Reynolds-number wall-bounded flows at any regime.

A. Wall-heat flux of laminar boundary layers

We first present the decomposition of the wall-heat flux in compressible self-similar laminar boundary layers with Mach numbers ranging between 2.5 and 10.9. Boundary layers at Mach number 10.9 have been studied experimentally on cold walls ($T_w/T_{ad} = 0.2$) at the Calspan-University of the Buffalo Research Center (Gnoffo et al., 2011) and via direct numerical simulations (Huang et al., 2022). The dynamic viscosity is related to the temperature through Sutherland's law (Stewartson, 1964). For a laminar boundary layer, the decomposition (4.1) simplifies to

$$
\bar{\mathscr{q}}_w = \underbrace{-\frac{Pr\mathcal{M}_\infty^2(\gamma - 1)}{s(x)} \int_0^\infty \frac{\mu}{T}\left(\frac{\mathrm{d}U}{\mathrm{d}\eta}\right)^2 \mathrm{d}\eta}_{\bar{\mathscr{q}}_u} + \underbrace{\frac{Pr}{s(x)} \int_0^\infty (T - 1)U\mathrm{d}\eta}_{\bar{\mathscr{q}}_{\theta^T}},
$$

$$\tag{4.4}$$

where $s(x) = \sqrt{2x/Re}$. Equation (4.4) can also be obtained by integrating the energy equation in Eq. (A3). For the case of a self-similar Blasius laminar boundary layer, identity (4.4) can be simplified by defining $\bar{\mathscr{q}}_{w,R} = s(x)\bar{\mathscr{q}}_w$. The effects of the streamwise co-ordinate and the Reynolds number are thus excluded, while information about the heat-transfer physics is retained.

The flow parameters used to study identity (4.4) are listed in Table I. Figures 2(a) and 2(b) present the dependence of $\mathrm{d}^2F/\mathrm{d}\eta^2|_{\eta=0}$

TABLE I. Free-stream and wall temperature conditions.

$\mathcal{M}_\infty$	T_∞^* (K)	T_{ad}^* (K)	T_w^*/T_{ad}^*
2.5	270.0	270.0	1.0
4.9	66.2	348.4	0.91
7.87	51.8	620.8	0.48
10.9	66.5	1500	0.2
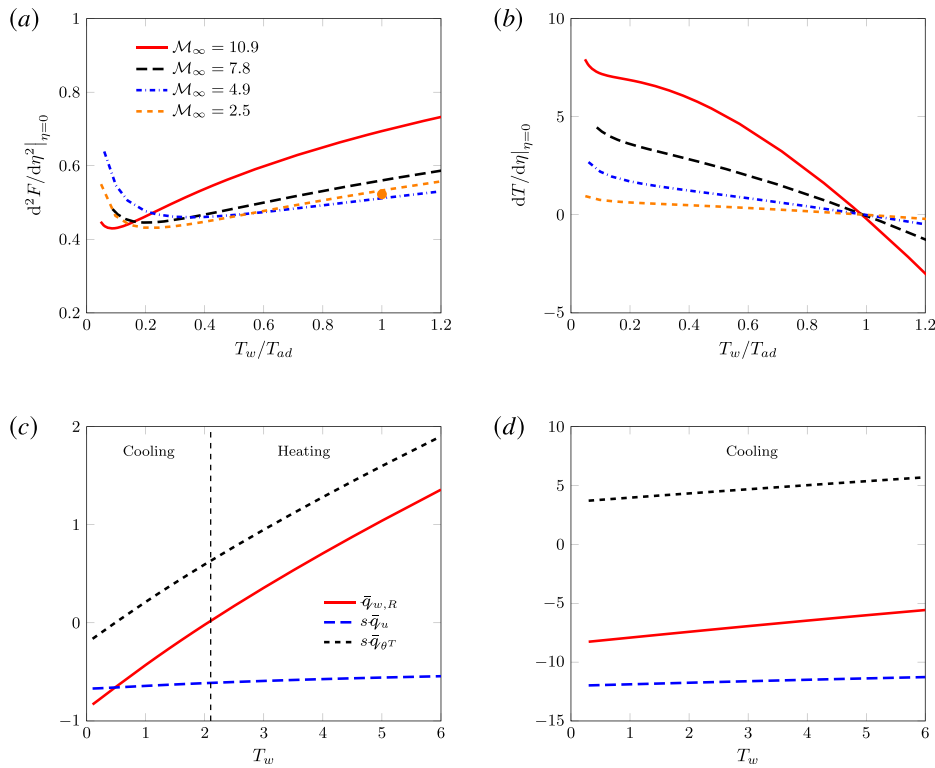
FIG. 2. (a) and (b) Dependence of $d^2F/d\eta^2|_{\eta=0}$ (a) and $dT/d\eta|_{\eta=0}$ (b) on the wall temperature ratio T_w/T_{ad}. The circle indicates the result of Xu *et al.* (2023), computed for $\mathcal{M}_\infty = 2.5$ and using power law for the dependence of the dynamic viscosity on the temperature, Stewartson (1964). (c) and (d) Decomposition of the wall-heat flux $\bar{q}_{w,R}$ at different wall temperatures for $Pr = 0.71$, $\gamma = 1.4$, $\mathcal{M}_\infty = 2.5$ (c), and $\mathcal{M}_\infty = 10.9$ (d).

and $dT/d\eta|_{\eta=0}$ on T_w/T_{ad}. The quantity $d^2F/d\eta^2|_{\eta=0}$ is influenced the most by T_w/T_{ad} for $\mathcal{M}_\infty = 10.9$. The gradient $dT/d\eta|_{\eta=0}$ grows significantly with the Mach number in the wall-cooling cases. Figures 2(c) and 2(d) display the decomposition of $\bar{q}_{w,R}$ for a supersonic case ($\mathcal{M}_\infty = 2.5$) and a hypersonic case ($\mathcal{M}_\infty = 10.9$), respectively. For $0 \leq T_w \leq 6$, wall cooling and wall heating are studied for $\mathcal{M}_\infty = 2.5$, while only wall cooling is studied for $\mathcal{M}_\infty = 10.9$. For both Mach numbers, the contribution of the dissipation term $s(x)\bar{q}_u$ depends only mildly on T_w, while the spatial-growth term $s(x)\bar{q}_{\theta^T}$ is more significantly influenced by T_w. In the wall-cooling cases, the spatial-growth term $s(x)\bar{q}_{\theta^T}$ opposes the wall-heat transfer (except for extremely low wall temperatures), while the dissipation term $s(x)\bar{q}_u$ increases the wall-heat transfer.
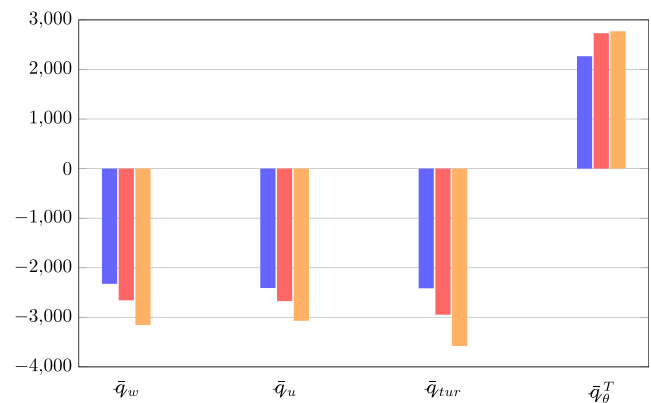
B. Wall-heat flux of turbulent boundary layers

The decomposition of the wall-heat flux for fully developed turbulent boundary layers is studied by using the direct numerical simulation data of Huang *et al.* (2022). We choose the local density boundary thickness $\delta^*_{\rho 99}$ as the reference length for this analysis, as explained in the Appendix. The Reynolds number is thus $R_\delta = \rho^*_\infty \delta^*_{\rho 99} \mathcal{U}^*_\infty / \mu^*_\infty$.

Figure 3 presents the magnitudes of the terms in the identity (4.1) at three Reynolds numbers for $\mathcal{M}_\infty = 10.9$ with a cooled wall. The terms $\bar{q}_u$ and $\bar{q}_{tur}$ dominate the balance and have the same sign of the wall-heat flux. Term $\bar{q}_{\theta^T}$ is instead opposed to the wall-heat flux. Over this range, the Reynolds number of the turbulent boundary layer only has a small impact on the relative contributions of each

term to the wall-heat flux. Figure 4 presents the magnitudes of the terms in the identity (4.1) at three Reynolds numbers at $\mathcal{M}_\infty = 2.5$ for vanishingly small wall-heat flux. The mean-flow dissipation and the turbulent kinetic energy production by the Favre–Reynolds stresses are neutralized by the growth of the thermal boundary layer.

Zhang and Xia (2020) reported that, for subsonic and supersonic channel flows with cooled walls, the energy dissipation into heat is also

FIG. 3. Decomposition of the heat-transfer coefficient $\bar{q}_w$ into the terms of Eq. (4.1) for turbulent boundary layers. The numerical data are from the direct numerical simulations by Huang *et al.* (2022) at $\mathcal{M}_\infty = 10.9$ (wall-cooling case). The Reynolds numbers are $R_\delta = 566\,533$ (blue), $R_\delta = 722\,422$ (red), and $R_\delta = 930\,733$ (yellow).
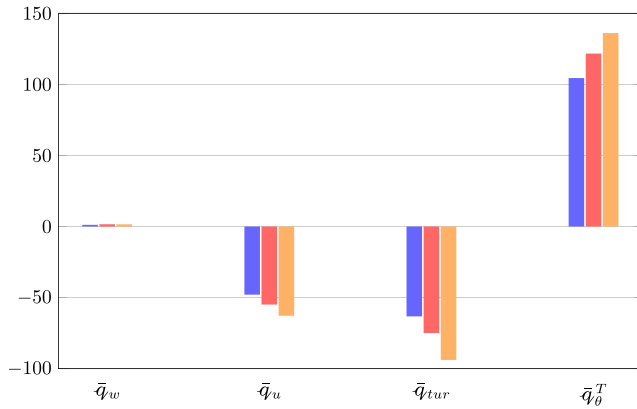
FIG. 4. Decomposition of the heat-transfer coefficient $\bar{q}_w$ into the terms of Eq. (4.1) for turbulent boundary layers. The numerical data are from the direct numerical simulations by Huang *et al.* (2022) at $\mathcal{M}_\infty = 2.5$ (adiabatic wall case). The Reynolds numbers are $R_\delta = 71\,606$ (blue), $R_\delta = 89\,863$ (red), and $R_\delta = 114\,564$ (yellow).

the dominant effect in the heat-transfer physics, although they did not separate the mean-flow dissipation and the turbulent dissipation from the total dissipation. Zhang and Xia (2020) also found that the dissipation term gives a 90% contribution to the total wall-heat flux because of the absence of the streamwise inhomogeneity in their channel-flow cases.

V. SIMPLIFICATION OF ALTERNATIVE FUKAGATA–IWAMOTO–KASAGI IDENTITIES

Barone *et al.* (2022) and Wenzel *et al.* (2022) showed that all the FIK-like identities for the skin-friction coefficient of free-stream boundary layers depend on the upper bound of integration. In this section, we study how the upper integration bound impacts the twofold identities derived by Wenzel *et al.* (2022) and Xu *et al.* (2022) for the decomposition of the wall-heat flux. We also investigate how the number of successive integrations used in the multifold identity derived by Wenzel *et al.* (2022) influences the relative contribution of the terms in the identity.

A. Simplification of the twofold Wenzel–Gibis–Kloker identity

Integrating the energy equation (2.8) from 0 to y and multiplying both sides by $R_\delta Pr$ lead to

$$R_\delta Pr \bar{\rho} \langle v'' T'' \rangle - \bar{\mu} \frac{\partial \bar{T}}{\partial y} + \mu_w \frac{\partial \bar{T}}{\partial y}\bigg|_{y=0}$$
$$+ R_\delta Pr \mathcal{M}_\infty^2 (\gamma - 1) \int_0^y \bar{\rho} \langle u'' v'' \rangle \frac{\partial \bar{u}}{\partial y} dy$$
$$- Pr \mathcal{M}_\infty^2 (\gamma - 1) \int_0^y \bar{\mu} \left(\frac{\partial \bar{u}}{\partial y}\right)^2 dy + R_\delta Pr \int_0^y H_x dy = 0, \quad (5.1)$$

where

$$H_x = \frac{\partial \bar{\rho} \langle T \rangle \langle u \rangle}{\partial x} + \frac{\partial \bar{\rho} \langle T \rangle \langle v \rangle}{\partial y}. \quad (5.2)$$

Integrating (5.1) from 0 to a wall-normal location h in the free stream, i.e., where $\overline{Tu} = 1$ and $\overline{Tv} = 0$, leads to

$$-h\mu_w \frac{\partial \bar{T}}{\partial y}\bigg|_{y=0} = R_\delta Pr \int_0^h \bar{\rho} \langle v'' T'' \rangle dy - \int_0^h \bar{\mu} \frac{\partial \bar{T}}{\partial y} dy$$
$$- Pr \mathcal{M}_\infty^2 (\gamma - 1) \int_0^h (h-y) \bar{\mu} \left(\frac{\partial \bar{u}}{\partial y}\right)^2 dy$$
$$+ R_\delta Pr \mathcal{M}_\infty^2 (\gamma - 1) \int_0^h (h-y) \bar{\rho} \langle u'' v'' \rangle \frac{\partial \bar{u}}{\partial y} dy$$
$$+ R_\delta Pr \int_0^h (h-y) H_x dy. \quad (5.3)$$

Dividing (5.3) by h leads to

$$\bar{q}_w = \underbrace{\frac{R_\delta Pr}{h} \int_0^h \bar{\rho} \langle v'' T'' \rangle dy}_{\text{Term 1}} - \underbrace{\frac{1}{h} \int_0^h \bar{\mu} \frac{\partial \bar{T}}{\partial y} dy}_{\text{Term 2}}$$
$$+ \underbrace{\frac{R_\delta Pr \mathcal{M}_\infty^2 (\gamma - 1)}{h} \int_0^h (h-y) \bar{\rho} \langle u'' v'' \rangle \frac{\partial \bar{u}}{\partial y} dy}_{\text{Term 3}}$$
$$- \underbrace{\frac{Pr \mathcal{M}_\infty^2 (\gamma - 1)}{h} \int_0^h (h-y) \bar{\mu} \left(\frac{\partial \bar{u}}{\partial y}\right)^2 dy}_{\text{Term 4}} + \underbrace{\frac{R_\delta Pr}{h} \int_0^h (h-y) H_x dy}_{\text{Term L}},$$
$$(5.4)$$

where the last term can be decomposed as follows:

$$\text{Term L} = \frac{R_\delta Pr}{h} \int_0^h (h-y) H_x dy = \underbrace{\frac{R_\delta Pr}{h} \int_0^h h H_x dy}_{\text{Term 5}} - \underbrace{\frac{R_\delta Pr}{h} \int_0^h y H_x dy}_{\text{Term 6}}.$$
$$(5.5)$$

The terms on the right-hand side of Eq. (5.4) depend on the integration bound h, as shown in Fig. 2 of Barone *et al.* (2022). There is no fixed rule on how to choose the upper integration bound h, except that it must correspond to a location where the mean-flow temperature matches the uniform free-stream temperature and the mean boundary-layer velocity matches the uniform and wall-parallel free-stream velocity.

Figure 5 presents the dependence of terms 1–6 in Eqs. (5.4) and (5.5) on the upper bound of integration. The vertical line denotes the location where the density is equal to 99% of the free-stream value. The heat-transfer coefficients obtained by the twofold integration identities, given by Eq. (A4) in WGK and by Eq. (3.9) in Xu *et al.* (2022), are based on the equations of total enthalpy and internal equations, respectively. The wall-heat flux is instead derived here by using the temperature equation. All the terms are found to depend heavily on the upper bound h. Terms 1 and 2 vanish when the upper bound h is large, which indicates that this limit rules out the turbulent heat flux and the mean-flow heat transfer from the identity. The remaining contributions are from term 3, involving the Favre–Reynolds stresses, term 4, related to the mean-flow velocity, and term 5, part of the non-homogeneous term. The present results are consistent with Fig. 16 of Barone *et al.* (2022). Their turbulent term I_{T_y} is our term 1 in which we neglect the high-order terms according to the boundary-layer assumption (White, 2006). The combination of terms I_{C_y} and I_{C_x} is

30 November 2023 14:34:50
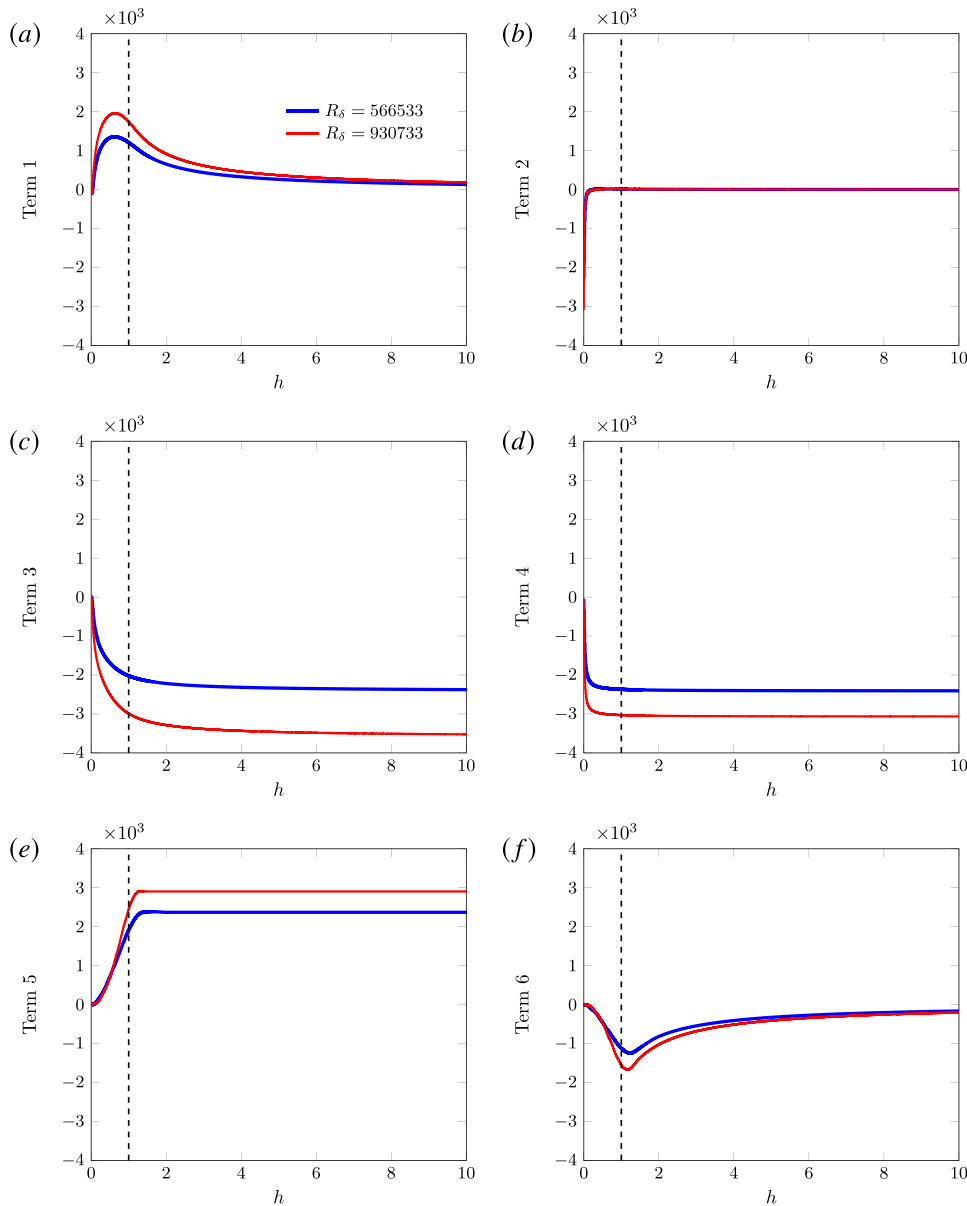
FIG. 5. Dependence of terms in Eq. (5.4) obtained by the twofold repeated integration on the upper integration bound h for the turbulent boundary layers: (a) term 1, (b) term 2, (c) term 3, (d) term 4, (e) term 5, and (f) term 6. The numerical data are from the direct numerical simulations by Huang et al. (2022) at $\mathcal{M}_\infty = 10.9$. The vertical line indicates the wall-normal locations where $h^* = \delta^*_{\rho 99}(h = 1)$.

equivalent to the sum of terms 5 and 6 here. As shown by Barone et al. (2022), if the upper bound of integration h becomes larger, term 1 decreases but the combination of I_{C_y} and I_{C_x} increases.

Figure 6(a) compares the contributions of the streamwise-inhomogeneous term L with that of the turbulent-heat-transport term 1, while Fig. 6(b) compares the contributions of the Favre–Reynolds-stress term 3 with that of the mean-flow dissipation term 4. As the upper integration bound increases, the turbulent-heat-transport term 1 increases when h is confined within the boundary layer, but it eventually drops as $h \to \infty$. The key observation is that this trend causes term 1 to be smaller than term L for $h = 1$ and larger than term L for $h = 2$, which means that the nonhomogeneous term L is dominant for large h. A similar crossover happens for the Favre–Reynolds-stress term 3 and

the mean-flow dissipation term 4 for the larger Reynolds number case. It follows that the upper integration bound h impacts qualitatively and quantitatively on the role of the terms on the wall-heat transfer. The crucial issue is that, since h is a mathematical quantity used to derive the identity, we conclude that the dependence of the terms on h is spurious.

Similar to the analysis by Ricco and Skote (2022) on the skin friction, the dependence of the heat flux on the upper bound of integration can also be removed by taking the upper bound h to be asymptotically large. In this limit, the twofold identity derived by Wenzel et al. (2022) reduces to our identity (4.1), as follows. Terms 1 and 2 on the right-hand side of Eq. (5.4) are null in the limit $h \to \infty$, because the integrals are finite as the components of the corresponding
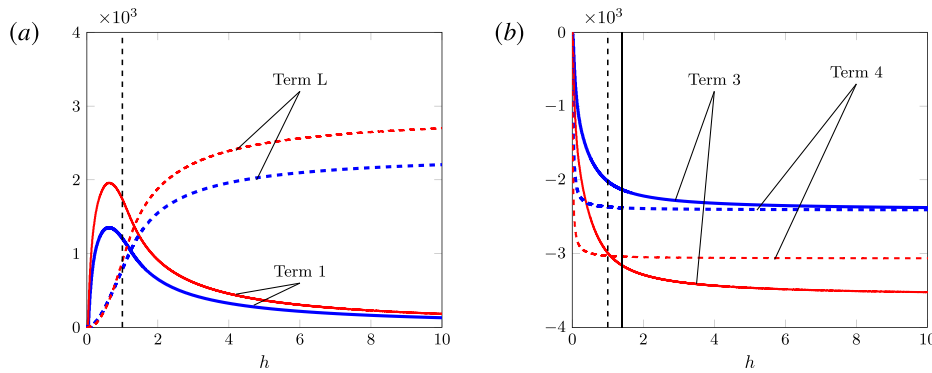
FIG. 6. (a) Comparison of the turbulent heat-transfer term 1 with the nonhomogeneous term L. (b) Comparison of the Favre–Reynolds stress term 3 with the mean-flow dissipation term 4. The numerical data are from the direct numerical simulations by Huang *et al.* (2022) at $\mathcal{M}_\infty = 10.9$. The vertical line indicates the wall-normal locations where $h^* = \delta^*_{\rho 99}(h = 1)$. The thin and solid lines correspond to the two Reynolds-number cases given in the legend of Fig. 5.

integrands, $\langle v''T''\rangle$ and $\partial \bar{T}/\partial y$, are zero in the free stream. As $h \to \infty$, term 3 in Eq. (5.4) simplifies to term $\bar{q}_{tur}$ in Eq. (4.1) and term 4 in Eq. (5.4) simplifies to term $\bar{q}_u$ in Eq. (4.1). In this limit, term 5 in Eq. (5.5) simplifies to term $\bar{q}_\theta^T$ in Eq. (4.1) because the term involving $\partial/\partial y$ in Eq. (5.2) is null due to the integration along y and $\partial/\partial x$ in the first term in Eq. (5.2), and can be taken outside of the integral.

B. Simplification of the multifold Wenzel–Gibis–Kloker identity

From the energy equation, Wenzel *et al.* (2022) obtained a heat-transfer identity by carrying out a number of successive integrations n between 0 and y performed before the final integration between 0 and h. In this section, we prove that the multifold identity reduces to the definition of the wall-heat flux when the number of integration is asymptotically large. The Reynolds number is again defined by using $\delta^*_{\rho 99}$.

The infinite number of successive integrations between 0 and y performed on Eq. (2.8) before the final integration between 0 and h leads to

$$\bar{q}_w = \underbrace{\frac{nR_\delta Pr}{h^n}\int_0^h (h-y)^{n-1}\rho\langle v''T''\rangle\,\mathrm{d}y}_{\text{Term I}} - \underbrace{\frac{n}{h^n}\int_0^h (h-y)^{n-1}\bar{\mu}\frac{\partial \bar{T}}{\partial y}\,\mathrm{d}y}_{\text{Term II}}$$

$$+ \underbrace{\frac{R_\delta Pr\mathcal{M}_\infty^2(\gamma-1)}{h^n}\int_0^h (h-y)^n\bar{\rho}\langle u''v''\rangle\frac{\partial \bar{u}}{\partial y}\,\mathrm{d}y}_{\text{Term III}}$$

$$- \underbrace{\frac{Pr\mathcal{M}_\infty^2(\gamma-1)}{h^n}\int_0^h (h-y)^n\bar{\mu}\left(\frac{\partial \bar{u}}{\partial y}\right)^2\,\mathrm{d}y}_{\text{Term IV}}$$

$$+ \underbrace{\frac{R_\delta Pr}{h^n}\int_0^h (h-y)^n H_x\,\mathrm{d}y}_{\text{Term V}}. \tag{5.6}$$

Figure 7 shows the heat flux terms I–V of Eq. (5.6) as a function of the integration number n. The integration upper bound is chosen as $h = 1$ ($h^* = \delta^*_{\rho 99}$). All the terms approach zero as the integration number n increases, except for term II, which is related to the mean-flow temperature. We now study the limit $n \to \infty$ of Eq. (5.6) for $h = 1$. We adapt the method of Xu *et al.* (2023) for the analysis of the skin-

friction coefficient to the wall-heat flux case. By using the change of variable $\xi = -\ln(1-y)$, the wall-heat flux becomes

$$\bar{q}_w = nR_\delta Pr\int_0^\infty \rho\langle v''T''\rangle e^{-n\xi}\,\mathrm{d}\xi - n\int_0^\infty \bar{\mu}\frac{\partial \bar{T}}{\partial y}e^{-n\xi}\,\mathrm{d}\xi$$

$$+ R_\delta Pr\mathcal{M}_\infty^2(\gamma-1)\int_0^\infty \bar{\rho}\langle u''v''\rangle\frac{\partial \bar{u}}{\partial y}e^{-\xi}e^{-n\xi}\,\mathrm{d}\xi$$

$$- Pr\mathcal{M}_\infty^2(\gamma-1)\int_0^\infty \bar{\mu}\left(\frac{\partial \bar{u}}{\partial y}\right)^2 e^{-\xi}e^{-n\xi}\,\mathrm{d}\xi$$

$$+ R_\delta Pr\int_0^\infty H_x e^{-\xi}e^{-n\xi}\,\mathrm{d}\xi. \tag{5.7}$$

We focus on the only term remaining in the limit $n \to \infty$, i.e., the second term on the right-hand side of Eq. (5.7), i.e., the mean-flow term II in Eq. (5.6). In the limit $\xi \to 0^+$,

$$\bar{\mu}\frac{\partial \bar{T}}{\partial y} \sim B_0 + B_1 y + B_2 y^2 + O(y^3)$$

$$= B_0 + B_1(1-e^{-\xi}) + B_2(1-e^{-\xi})^2 + \cdots$$

$$= B_0 + B_1\xi + \left(B_2 - \frac{B_1}{2}\right)\xi^2 + O(\xi^3). \tag{5.8}$$

The coefficient $B_n(R_\delta)$ can be determined numerically. Using Watson's lemma (Bender *et al.*, 1999) leads to

$$\bar{q}_w \sim \cdots - n\left[\frac{\Gamma(1)B_0}{n} + \frac{\Gamma(2)B_1}{n^2} + \left(B_2 - \frac{B_1}{2}\right)\frac{\Gamma(3)}{n^3} + \cdots\right]$$

$$\sim -B_0 \sim -\bar{\mu}_w\frac{\partial \bar{T}}{\partial y}\bigg|_{y=0}, \tag{5.9}$$

where Γ is the Gamma function. As n grows, the wall-heat flux approaches B_0, that is, the mean-flow temperature term II in Eq. (5.6) is found to be asymptotically equal to the wall-heat flux when $n \to \infty$, ruling out the contributions of the turbulent heat flux, the Favre–Reynolds stresses, the mean-flow dissipation, and the nonhomogeneous effects. As the identity collapses to the definition of the wall-heat flux itself, no information is revealed about the heat-transfer physics, proving that the dependence on n is spurious.

VI. CONCLUSIONS

We have studied integral formulas for the decomposition of the wall-heat flux of high-Reynolds-number compressible boundary
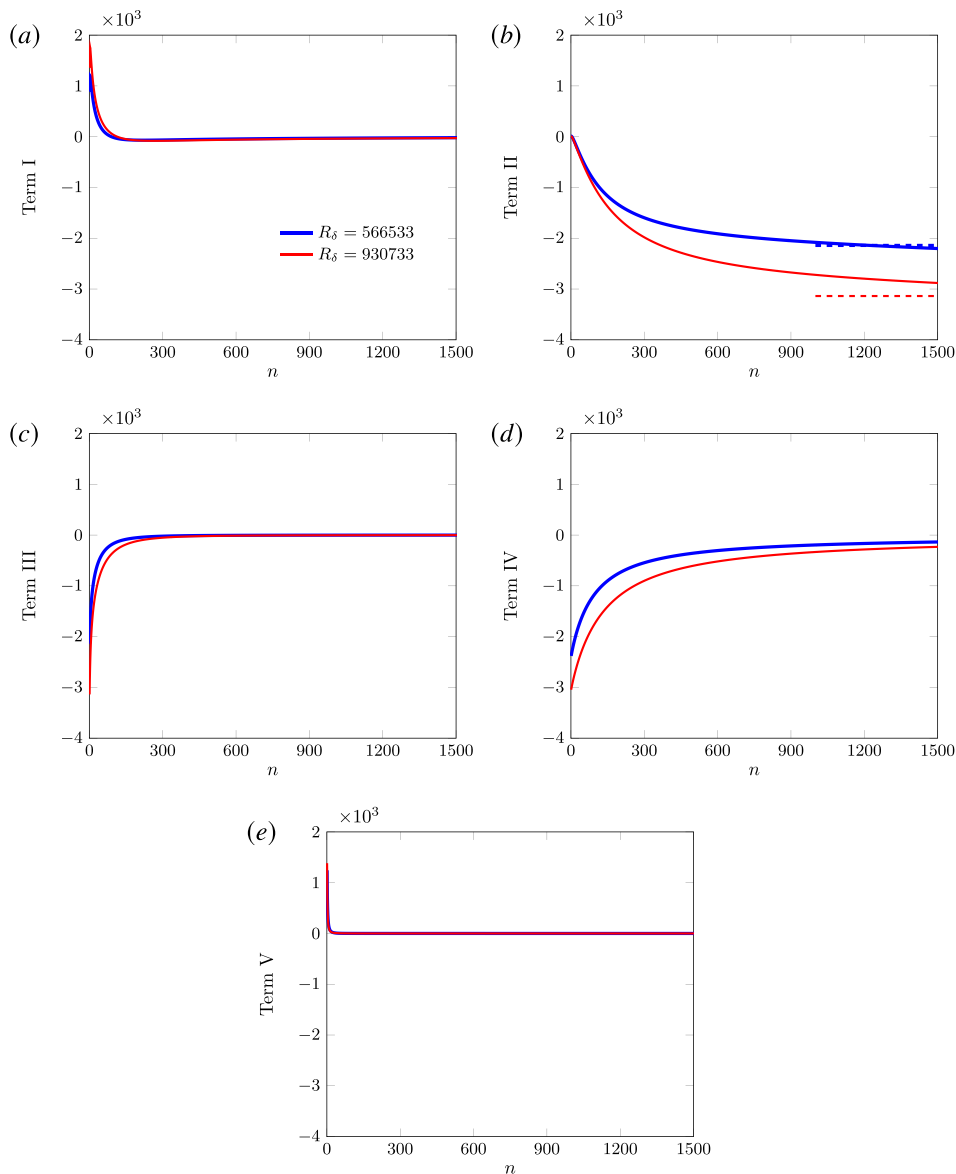
FIG. 7. Dependence of terms in Eq. (5.6) obtained by multifold repeated integration on the integration number n for the turbulent boundary layers: (a) term I, (b) term II, (c) term III, (d) term IV, and (e) term V. The numerical data are from the direct numerical simulations by Huang et al. (2022) at $\mathcal{M}_\infty = 10.9$. The dashed lines indicate the corresponding local total heat flux.

layers. The theoretical approach used to derive the identities of Elnahhas and Johnson (2022) and Xu et al. (2023) for the decomposition of the skin-friction coefficient was utilized to obtain an integral identity for the wall-heat flux that isolates the contributions of the laminar wall-heat flux and the turbulent heat transport. We discussed the physical meaning of the decomposition terms and the limitations of the identity, focusing on adiabatic-wall and wall-cooling cases.

A simplified integral identity for the decomposition of the wall-heat flux was obtained by direct integration of the mean temperature equation. This identity is the heat-transfer analog to the von Kármán momentum integral equation for the wall friction and it was used for the first time to study compressible laminar and turbulent boundary layers. It can be used in experimental studies on supersonic and hypersonic boundary layers to obtain the wall-heat flux. For boundary layers

at Mach 2.5 with an adiabatic wall and at Mach 10.9 with a cooled wall, the thermal balance is dominated by the production of turbulent kinetic energy, ruled by the Favre–Reynolds stresses, and by the mean-flow dissipation. The mean-flow streamwise inhomogeneity was instead found to oppose the wall cooling. The absolute values of all the terms in the identity increase with the Reynolds number.

We have also shown that, in the twofold integration identities discovered by Wenzel et al. (2022) and Xu et al. (2022), the upper integration bound used in those studies has a significant impact on the terms of the identities. Being the bound a mathematical quantity, it follows that the dependence of the identity on this bound is nonphysical. This problem prevents the use of these identities for the quantification of the effects of the Favre–Reynolds stresses and the turbulent heat transport on the wall-heat flux. In the limit of a large integration

bound, these identities simplify to our direct-integration heat-transfer identity. The multifold integration identity proposed by Wenzel *et al.* (2022) was also investigated. We have theoretically and numerically proved that, as the number of integration becomes asymptotically large, this multifold identity degenerates to the definition of the wall-heat flux thus uncovering no information about the boundary-layer physics and leading to the conclusion that the dependence of the multifold identity on the number of integrations is spurious.

ACKNOWLEDGMENTS

AUTHOR DECLARATIONS
Conflict of Interest

The authors have no conflicts to disclose.

Author Contributions

Dongdong Xu: Conceptualization (equal); Data curation (equal); Formal analysis (equal); Investigation (equal); Methodology (equal); Software (equal); Validation (equal); Writing – original draft (equal); Writing – review & editing (equal). **Pierre Ricco:** Conceptualization (equal); Data curation (equal); Formal analysis (equal); Funding acquisition (equal); Investigation (equal); Methodology (equal); Supervision (equal); Validation (equal); Writing – original draft (equal); Writing – review & editing (equal). **Lian Duan:** Conceptualization (equal); Funding acquisition (equal); Investigation (equal); Methodology (equal); Writing – original draft (equal); Writing – review & editing (equal).

DATA AVAILABILITY

Data sharing is not applicable to this article as no new data were created or analyzed in this study.

APPENDIX: DERIVATION OF INTEGRAL IDENTITY (3.2)

The mathematical derivation of Eq. (3.2) is presented. It is first instructive to detail the mathematical framework for the laminar boundary layer. The compressible Blasius boundary layer without a streamwise pressure gradient possesses a similarity solution (Stewartson, 1964),

$$u = U = F'(\eta), \quad v = \frac{T(\eta_c F' - F)}{\sqrt{2xRe}}, \quad T = T(\eta), \quad \text{(A1)}$$

where $\eta_c = T^{-1} \int_0^\eta T(\check{\eta}) \mathrm{d}\check{\eta}$, and the similarity variable η is

$$\eta = \sqrt{\frac{Re}{2x}} \int_0^y \rho(x, \check{y}) \mathrm{d}\check{y}. \quad \text{(A2)}$$

The prime denotes differentiation with respect to η. The compressible Blasius functions $F(\eta)$ and $T(\eta)$ are determined by the boundary-value problem,

$$(\mu F''/T)' + FF'' = 0,$$
$$(\mu T'/T)' + PrFT' + \mu(\gamma - 1)Pr\mathcal{M}_\infty^2 (F'')^2/T = 0,$$
$$F = F' = 0, \quad T = T_w \quad \text{at} \quad \eta = 0, \quad \text{(A3)}$$
$$F' = 1, \quad T' = 0, \quad \text{as} \quad \eta \to \infty,$$

where the Prandtl number $Pr = 0.71$. The dynamic viscosity is described by Sutherland's law (Stewartson, 1964) in the numerical computations, although the theory is valid for any viscosity law. The wall is isothermal as the wall temperature T_w is constant.

The following mathematical steps are used in the derivation of Eq. (3.2):

- Heat conduction and laminar heat flux,

$$\frac{1}{RePr} \int_0^\infty (y - \mathcal{L}) \frac{\partial}{\partial y} \left(\bar{\mu} \frac{\partial \bar{T}}{\partial y} \right) \mathrm{d}y$$

$$= \frac{1}{RePr} \left(\mathcal{L} \mu_w \frac{\partial \bar{T}}{\partial y} \bigg|_{y=0} - \int_0^\infty \bar{\mu} \frac{\partial \bar{T}}{\partial y} \mathrm{d}y \right)$$

$$= \frac{1}{RePr} \left(\mathcal{L} \mu_w \frac{\partial \bar{T}}{\partial y} \bigg|_{y=0} - (1 - \mu_w T_w) + \int_0^\infty \frac{\partial \bar{\mu}}{\partial y} \bar{T} \mathrm{d}y \right)$$

$$= \frac{\mathcal{L}}{RePr} \left(-\bar{q}_w - \frac{1}{\mathcal{L}} + \frac{\mu_w T_w}{\mathcal{L}} + \int_0^\infty \frac{1}{\mathcal{L}} \frac{\partial \bar{\mu}}{\partial y} \bar{T} \mathrm{d}y \right). \quad \text{(A4)}$$

The first term on the last line of Eq. (A4) is used to obtain the wall-heat flux. The second term in Eq. (A4) is utilized to isolate the laminar contribution. The third and fourth terms in Eq. (A4) are included in the term related to the viscosity. We choose an appropriate $\mathcal{L}$ for the wall-heat flux,

$$\bar{q}_w = \bar{q}_l = -\frac{1}{\mathcal{L}} = -\frac{\mathcal{G}(\mathcal{M}_\infty, T_w)}{\sqrt{Re_x}} = -\mu_w \frac{\partial T}{\partial y} \bigg|_{y=0} = -\frac{\mu_w}{sT_w} \frac{\mathrm{d}T}{\mathrm{d}\eta} \bigg|_{\eta=0}. \quad \text{(A5)}$$

The wall-heat flux of self-similar boundary layers is given by Eq. (6.77) of Anderson (2000). The laminar contribution is isolated from the wall-heat flux (A5) by choosing $\mathcal{L}(x)$ as given in Eq. (3.6):

- Favre–Reynolds stresses,

$$\mathcal{M}_\infty^2 (\gamma - 1) \int_0^\infty (y - \mathcal{L}) \bar{\rho} \langle u'' v'' \rangle \frac{\partial \bar{u}}{\partial y} \mathrm{d}y$$

$$= -\mathcal{L} \mathcal{M}_\infty^2 (\gamma - 1) \int_0^\infty \left(1 - \frac{y}{\mathcal{L}} \right) \bar{\rho} \langle u'' v'' \rangle \frac{\partial \bar{u}}{\partial y} \mathrm{d}y. \quad \text{(A6)}$$

- Turbulent heat-flux contribution,

$$\int_0^\infty (y - \mathcal{L}) \frac{\partial \bar{\rho} \langle T'' v'' \rangle}{\partial y} \mathrm{d}y = -\mathcal{L} \int_0^\infty \frac{1}{\mathcal{L}} \bar{\rho} \langle T'' v'' \rangle \mathrm{d}y. \quad \text{(A7)}$$

- Mean-flow dissipation,

$$\int_0^\infty (\mathcal{L} - y) \frac{1}{Re} \bar{\mu} \left(\frac{\partial \bar{u}}{\partial y} \right)^2 \mathrm{d}y = \mathcal{L} \int_0^\infty \left(1 - \frac{y}{\mathcal{L}} \right) \frac{1}{Re} \bar{\mu} \left(\frac{\partial \bar{u}}{\partial y} \right)^2 \mathrm{d}y. \quad \text{(A8)}$$

- Streamwise convection,

$$\int_0^\infty (y - \mathscr{L}) \frac{\partial(\langle T \rangle - 1)\bar{\rho}\langle u \rangle}{\partial x} \mathrm{d}y$$
$$= -\mathscr{L}(T_w - 1)\left(\frac{\mathrm{d}\theta_{\mathscr{L}}^T}{\mathrm{d}x} - \frac{\theta^T - \theta_{\mathscr{L}}^T}{\mathscr{L}} \frac{\mathrm{d}\mathscr{L}}{\mathrm{d}x}\right), \qquad (A9)$$

where θ^T and $\theta_{\mathscr{L}}^T$ are given in Eqs. (3.3) and (3.4), respectively.

- Wall-normal convection,

$$\int_0^\infty (y - \mathscr{L}) \frac{\partial(\langle T \rangle - 1)\bar{\rho}\langle v \rangle}{\partial y} \mathrm{d}y = -\mathscr{L}(T_w - 1)\frac{\theta_v^T}{\mathscr{L}}, \qquad (A10)$$

where θ_v^T is shown in Eq. (3.5).

The identity (3.2) is related to the identity (4.1). In the limit $\mathscr{L} \to \infty$, terms $\bar{q}_l$, $\bar{q}_{\bar{\mu}}$, $\bar{q}_h$, and $\bar{q}_{\theta_v^T}$ are null, while terms $\theta_{\mathscr{L}}^T$ reduces to the momentum thickness since $y/\mathscr{L} \ll 1$. The term $\bar{q}_{\theta^T}$ simplifies to $\mathrm{d}\theta^T/\mathrm{d}x$ because the second term of $\bar{q}_{\theta^T}$ is null. The enthalpy thickness can be eliminated so that, for $\mathscr{L} \to \infty$, Eq. (3.2) simplifies to Eq. (4.1).

In order to compare the wall-heat flux of a laminar boundary layer with that of a turbulent boundary layer, a reference physical quantity should be fixed for both flows, as in the incompressible case studied by EJ for the skin friction. This reference length can be the streamwise location x, the thermal displacement thickness, the thermal momentum thickness, or the thermal boundary-layer thickness $\delta_{\rho 99}$, i.e., the wall-normal distance where the streamwise mean density reaches 99% of the free-stream density. We choose the thermal momentum thickness $\delta_{\rho 99}^*$ as the reference scale for our analysis. It follows that we compare the wall-heat flux of a laminar flow with that of a turbulent flow for the same thermal thickness. The thermal thickness is a better choice than the streamwise location x because a fully developed turbulent boundary layer may be induced artificially at different streamwise locations. The streamwise location x is obtained by the relation

$$\delta_{\rho 99} = \sqrt{\frac{2x}{R_\delta}} \int_0^{\eta_{99}} T \mathrm{d}\eta = 1, \qquad (A11)$$

where R_δ is the Reynolds number defined by $\delta_{\rho 99}^*$, and η_{99} is the wall-normal location where $\rho = 0.99$. $\mathscr{L}(x)$ is finally computed by Eq. (3.6).

REFERENCES

Adumitroaie, V., Ristorcelli, J. R., and Taulbee, D. B., "Progress in Favré–Reynolds stress closures for compressible flows," Phys. Fluids **11**(9), 2696–2719 (1999).

Anderson, J. D., *Hypersonic and High Temperature Gas Dynamics*, AIAA-Education Series, 2nd ed. (AIAA, 2000).

Andreopoulos, Y. and Honkan, A., "An experimental study of the dissipative and vortical motion in turbulent boundary layers," J. Fluid Mech. **439**, 131–163 (2001).

Barone, M., Nicholson, G. L., and Duan, L., "Internal energy balance and aerodynamic heating predictions for hypersonic turbulent boundary layers," Phys. Rev. Fluids **7**(8), 084604 (2022).

Bender, C. M., Orszag, S., and Orszag, S. A., *Advanced Mathematical Methods for Scientists and Engineers I: Asymptotic Methods and Perturbation Theory*, 1st ed. (Springer Science & Business Media, New York, 1999).

Elnahhas, A. and Johnson, P. L., "On the enhancement of boundary layer skin friction by turbulence: An angular momentum approach," J. Fluid Mech. **940**, A36 (2022).

Fan, Y., Li, W., and Pirozzoli, S., "Energy exchanges in hypersonic flows," Phys. Rev. Fluids **7**(9), L092601 (2022).

Favre, A. J., "The equations of compressible turbulent gases," Technical Report No. AD0622097 (DTIC Document, 1965).

Favre, A. J., "Formulation of the statistical equations of turbulent flows with variable density," in *Studies in Turbulence* (Springer, 1992), pp. 324–341.

Fukagata, K., Iwamoto, K., and Kasagi, N., "Contribution of Reynolds stress distribution to the skin friction in wall-bounded flows," Phys. Fluids **14**(11), L73–L76 (2002).

Gnoffo, P., Berry, S., and Van Norman, J., "Uncertainty assessments of 2D and axisymmetric hypersonic shock wave-turbulent boundary layer interaction simulations at compression corners," AIAA Paper No. AIAA 2011-3142, 2011.

Gomez, T., Flutet, V., and Sagaut, P., "Contribution of Reynolds stress distribution to the skin friction in compressible turbulent channel flows," Phys. Rev. E **79**(3), 035301 (2009).

Goyne, C., Stalker, R., and Paull, A., "Skin-friction measurements in high-enthalpy hypersonic boundary layers," J. Fluid Mech. **485**, 1–32 (2003).

Hopkins, E. J. and Inouye, M., "An evaluation of theories for predicting turbulent skin friction and heat transfer on flat plates at supersonic and hypersonic Mach numbers," AIAA J. **9**(6), 993–1003 (1971).

Huang, J., Duan, L., and Choudhari, M. M., "Direct numerical simulation of hypersonic turbulent boundary layers: Effect of spatial evolution and Reynolds number," J. Fluid Mech. **937**, A3 (2022).

Kays, W. and Crawford, M., *Convective Heat and Mass Transfer*, 3rd ed. (McGraw Hill, Inc., 1993).

Kianfar, A., Di Renzo, M., Williams, C., Elnahhas, A., and Johnson, P., "An angular momentum integral equation for high-speed boundary layers," in *Proceedings of the Summer Program 2022* (Center for Turbulence Research, 2022a).

Kianfar, A., Elnahhas, A., and Johnson, P. L., "Quantifying how turbulent fluctuations enhance skin friction and surface heat transfer in boundary layers," AIAA Paper No. AIAA 2022-0944 (2022b).

Lapsa, A. and Dahm, W., "Stereo particle image velocimetry of nonequilibrium turbulence relaxation in a supersonic boundary layer," Exp. Fluids **50**, 89–108 (2011).

Renard, N. and Deck, S., "A theoretical decomposition of mean skin friction generation into physical phenomena across the boundary layer," J. Fluid Mech. **790**, 339–367 (2016).

Ricco, P. and Skote, M., "Integral relations for the skin-friction coefficient of canonical flows," J. Fluid Mech. **943**, A50 (2022).

Roy, C. J. and Blottner, F. G., "Review and assessment of turbulence models for hypersonic flows," Prog. Aerosp. Sci. **42**(7–8), 469–530 (2006).

Schlichting, H. and Gersten, K., *Boundary-Layer Theory* (Springer, 2016).

Smits, A. J. and Dussauge, J. P., *Turbulent Shear Layers in Supersonic Flow* (Springer Science & Business Media, 2006).

Spalding, D. B. and Chi, S. W., "The drag of a compressible turbulent boundary layer on a smooth flat plate with and without heat transfer," J. Fluid Mech. **18**(1), 117–143 (1964).

Stewartson, K., *The Theory of Laminar Boundary Layers in Compressible Fluids* (Clarendon Press, Oxford, 1964).

Sun, D., Guo, Q., Yuan, X., Zhang, H., Li, C., and Liu, P., "A decomposition formula for the wall heat flux of a compressible boundary layer," Adv. Aerodyn. **3**(1), 1–13 (2021).

Tong, F., Dong, S., Lai, J., Yuan, X., and Li, X., "Wall shear stress and wall heat flux in a supersonic turbulent boundary layer," Phys. Fluids **34**(1), 015127 (2022a).

Tong, F., Yuan, X., Lai, J., Duan, J., Sun, D., and Dong, S., "Wall heat flux in a supersonic shock wave/turbulent boundary layer interaction," Phys. Fluids **34**(6), 065104 (2022b).

Van Driest, E. R., "Turbulent boundary layer in compressible fluids," J. Aeronaut. Sci. **18**(3), 145–160 (1951).

Van Driest, E. R., *The Problem of Aerodynamic Heating* (Institute of the Aeronautical Sciences, 1956).

Wenzel, C., Gibis, T., and Kloker, M., "About the influences of compressibility, heat transfer and pressure gradients in compressible turbulent boundary layers," J. Fluid Mech. **930**, A1 (2022).

White, F. M., *Viscous Fluid Flow* (McGraw-Hill, New York, 2006).

Xu, D., Ricco, P., and Duan, L., "Decomposition of the skin-friction coefficient of compressible boundary layers," Phys. Fluids **35**, 035107 (2023).

Xu, D., Wang, J., and Chen, S., "Skin-friction and heat-transfer decompositions in hypersonic transitional and turbulent boundary layers," J. Fluid Mech. **941**, A41 (2022).

Zhang, P. and Xia, Z., "Contribution of viscous stress work to wall heat flux in compressible turbulent channel flows," Phys. Rev. E **102**(4), 043107 (2020).

Zhang, C., Duan, L., and Choudhari, M. M., "Direct numerical simulation database for supersonic and hypersonic turbulent boundary layers," AIAA J. **56**(11), 4297–4311 (2018).

Zhang, P., Song, Y., and Xia, Z., "Exact mathematical formulas for wall-heat flux in compressible turbulent channel flows," Acta Mech. Sin. **38**(1), 1–10 (2022).